THE JOURNAL OF PHYSICAL CHEMISTRY B

Article

pubs.acs.org/JPCB

Influence of Solvent on Polymer Prequaternization toward Anion-Conductive Membrane Fabrication for All-Vanadium Flow Battery

Fengxiang Zhang,* Huamin Zhang,* and Chao Qu

Center for Energy Storage Batteries and Technologies, Dalian Institute of Chemical Physics, Chinese Academy of Sciences, China 457, Zhongshan Road, Dalian, China 116023

ABSTRACT: Triethylamine- (TEA-) enabled prequaternization of a polymer for nonalkaline anion-exchange membrane (AEM) fabrication is more facile and environmentally benign than the conventional trimethylamine-based postquaternization route. It is also more compatible with forming a microphase-separated membrane morphology that can facilitate ion transport. However, most studies of TEA-quaternized AEMs have reported unsatisfactory conductivities, and no examples of their application in all-vanadium flow batteries (VFBs) have been reported. In this work, we aim to address this issue and demonstrate that, by employing a favorable solvent, polysulfone can be prequaternized to a high level with TEA and further fabricated into an AEM showing good conductivity (18.2 mS cm^{-1} at room temperature) and impressive VFB performance (Coulombic efficiency above 98% and energy efficiency above 80% at 80 mA cm^{-2}). In contrast, when an unfavorable solvent is used, membrane quaternization does not occur significantly. This contrast is shown to result from the absence or presence of solvent−TEA competition during quaternization, which is related to the the electron-donating or -withdrawing properties of the solvents used. Our study adds new understanding to the quaternization chemistry of AEMs and also represents the first example, to our knowledge, of a TEA-quaternized AEM yielding high VFB efficiencies.

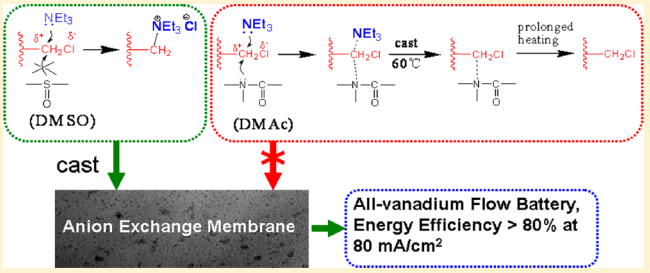

1. INTRODUCTION

The all-vanadium redox flow battery (VFB) can potentially circumvent the mismatch between the generation and end use of renewable but unsteady energies such as photovoltaics and wind turbines.[1] It is an electrochemical energy storage battery based on the redox reactions of different vanadium ions in the anolyte and catholyte solutions, which are separated by a membrane between them. The membrane transports H^+ or SO_4^{2-}/HSO_4^- ions for charge balance during battery operation and, more importantly, prevents admixing of vanadium ions from the two electrolytes. Currently, the state-of-the-art membrane for VFB is Nafion; it is excellent in terms of conductivity and stability but disadvantageous because of its high cost and low ion selectivity (caused by vanadium crossover through the membrane). Therefore, many efforts have been made to develop substitutes for Nafion such as aromatic polymer proton-exchange membranes[2,3] and nanoparticle or hybrid polyacid incorporated composite membranes.[4,5] Our past efforts in this regard have been focused on Nafion modification[6] or blending[7] and development of sulfonated polyetheretherketone membranes[8] and hydrocarbon nanofiltration membranes.[9] Most of these membranes, however, are still proton-conducting in nature and thus do not inherently reject vanadium ions, given that vanadium ions and protons both bear positive charges.

Use of an anion-exchange membrane (AEM) as a VFB separator might avoid vanadium crossover better than Nafion. This is because AEMs bear positive charges and thus can inherently repulse vanadium through the Donnan effect.[10,11] AEMs are typically fabricated by treating preformed, chloro- or bromomethylated polymer membranes with an aqueous solution of trimethylamine (TMA) to render the membrane functionalized with quaternary ammonium cations.[11−21] This is often a heterogeneous, postquaternization process, where quaternization is achieved by the gradual diffusion of TMA into the preformed membrane. In addition to the strong toxicity of TMA, the postquaternized membranes often suffer nonuniformity and deformation problems related to both the chloro- or bromomethylation degree of the precursory membrane and the rate of TMA diffusion. Also, these membranes lack a microphase-segregated morphology; microphase aggregation is able to produce continuous ion channels in the membrane and thus facilitate ion transport.[22−29]

Prequaternizing a polymer with a nontoxic or less toxic aminating reagent might constitute a straightforward solution for these issues. In this regard, triethylamine (TEA) is advantageous over TMA because of the former's good miscibility with polymer solutions, which enables prequaternization and further casting for membrane formation. TEA is also less toxic and more basic than TMA (pK_a = 10.65 and 9.76, respectively[30]) and has been used for AEM fabrication. However, such AEMs mostly exhibit low water sorption and low ion-exchange efficiency (IEC) and/or conductivity

Received: May 20, 2012
Revised: July 8, 2012
Published: July 9, 2012

dx.doi.org/10.1021/jp304880r | J. Phys. Chem. B 2012, 116, 9016−9022

according to the literature,[31−34] and no demonstration of their application in high-efficiency VFBs has been achieved.

Herein, we show that the prequaternization reaction with TEA is strongly influenced by the solvent employed for this reaction: With a favorable solvent such as dimethylsulfoxide, quaternization can reach a significant level, and the resultant membrane can exhibit high conductivity. When other solvents were used, however, only negligible quaternization resulted, and the membrane's ion-exchange properties were very low. We also carried out physical and chemical investigations into this quaternization difference. Our investigations suggest that solvents with an electron-donating propensity might compete with TEA during the target quaternization reaction between TEA and $-CH_2Cl$, leading to the failure of AEM fabrication. Such an adverse competition does not exist with a more electron-withdrawing solvents, so that quaternization can proceed to a high level. Finally, we studied the VFB performance of the successfully prequaternized AEM and found that it could yield a Coulombic efficiency of 99% and an energy efficiency 81% at a high charge/discharge current density (80 mA/cm^2), which are both relatively high among the literature-reported results for AEM-based VFBs operating under similar conditions.

2. EXPERIMENTAL SECTION

2.1. AEM Fabrication. AEMs were fabricated by TEA-enabled prequaternization of chloromethylated polysulfone (CMPSf). For CMPSf synthesis, 5 g of polysulfone (Udel P3500, Solvay) was dissolved in 200 mL of chloroform (analytical grade, stored in the presence of 4-Å molecular sieve) in a three-necked round-bottom flask. Upon complete dissolution of the polymer, 300 μL of anhydrous tin chloride ($SnCl_4$) was added under a nitrogen atmosphere and stirred at room temperature. Next, 8.5 mL of chloromethyl methyl ether (99%) was added slowly, and the mixture was stirred at 50−55 °C for 14 h. The resulting mixture was precipitated in rigorously stirred methanol, kept stirring for 12 h, and filtered and washed repeatedly with methanol. The obtained white solid, CMPSf, was vacuum-dried at 50 °C for 24 h; its degree of chloromethylation was determined to be 1.35 (chloromethyl groups per repeat unit of PSf) following our previously reported method.[35]

For membrane fabrication, CMPSf solutions (5%, w/v) were prepared with different solvents including dimethyl sulfoxide (DMSO), dimethylacetamide (DMAc), tetrahydrofuran (THF), and dimethylformamide (DMF). To each of these solutions, TEA was added in slight excess relative to the number of moles of chloromethyl groups. After being stirred at 30 °C for 20 h, the resulting solution was cast on a precleaned glass substrate and heated in the open air at 60 °C for 24 h to eliminate the solvent and unreacted TEA. For comparison purposes, another AEM was fabricated following the post-quaternization route, where a preformed CMPSf membrane was treated in a 30% trimethyamine (TMA) solution (aqueous) at room temperature for 15 h; the membrane was then soaked and rinsed repeatedly with deionized (DI) water to remove the unreacted TMA.

2.2. Membrane Characterizations. *2.2.1. Water Uptake (WU).* A dried membrane sample with known weight (W_0) was soaked in DI water for 24 h. The sample was then removed from the water; surface water was absorbed with a piece of filter paper; and the sample was weighed again, giving the new weight result (W). The water uptake (WU) was then calculated as

$$\mathrm{WU} = \frac{W - W_0}{W_0} \times 100\%$$

2.2.2. Ion-Exchange Capacity (IEC). The ion-exchange capacities (IECs) of membranes were determined using a titration-based method. Specifically, a membrane sample was first rendered into hydroxide form by being soaked in a 0.5 M NaOH solution at room temperature for 24 h. It was then equilibrated with deionized (DI) water in a sealed beaker for at least 24 h and rinsed copiously to remove physisorbed hydroxide ions. The soaking treatments were carried out using a carefully sealed container to minimize membrane carbonation with the ambient carbon dioxide. The treated membrane was soaked in a known volume of 0.01 M hydrochloric acid (HCl) for 48 h. The HCl solution was then titrated against 0.01 M NaOH (aqueous) with phenolphthalein as an indicator. The IEC was calculated as

$$\mathrm{IEC} = \frac{M_1V_1 - M_2V_2}{m}$$

where M_1 and V_1 denote the concentration and volume, respectively, of HCl solution before titration; M_2 and V_2 are the concentration and volume, respectively, of NaOH solution consumed in titration; and m is the mass of the dried membrane sample.

2.2.3. Conductivity. Ionic conductivity was measured by four-probe electrochemical impedance spectroscopy (EIS) using Solartron electrochemical equipment (S1287) over the frequency range from 5 MHz to 0.1 Hz. Before measurement, each membrane sample was soaked in DI water for at least 24 h and rinsed repeatedly to remove any physisorbed ions. It was then spanned between the two copper electrodes of an in-house-made testing fixture, with some DI water added to the small chamber housing the membrane sample. The membrane conductivity (σ, S cm^{-1}) was calculated as

$$\sigma = \frac{d}{RA}$$

where d is the distance between two electrodes (cm), A is the cross-sectional area of the membrane (cm^2), and R is the membrane resistance obtained from EIS (Ω). When R exceeds or approaches that of the DI water used, the membrane conductivity was regarded as undetectable.

2.2.4. Transmission Electron Microscopy (TEM). The membrane was stained with $PdCl_4^{2-}$ by overnight immersion in a large excess of 0.1 M H_2PdCl_4 aqueous solution. It was then rinsed copiously with deionized (DI) water, soaked in DI water overnight, and finally dried at room temperature for 12 h. The stained sample was embedded in epoxy resin and sliced into thin pieces by ultramicrotome with a diamond knife; the thin pieces were placed on copper grids for TEM study. TEM images were recorded on a JEOL JEM-2011 transmission electron microscope at an accelerating voltage of 120 kV.

2.2.5. Fourier Transform Infrared (FTIR) Spectroscopy. FTIR study of the membranes was performed using a JASCO FT-IR 4100 spectrometer in transmission mode. FTIR spectra were recorded in the wavenumber range of 400−4000 cm^{-1} with a resolution of 4 cm^{-1}.

2.2.6. Vanadium (VO^{2+}) Permeability. A diffusion cell consisting of two reservoirs separated by a membrane (Scheme

dx.doi.org/10.1021/jp304880r | J. Phys. Chem. B 2012, 116, 9016−9022

1) was constructed. The left reservoir was filled with 1.5 mol L^{-1} $VOSO_4$ in 3 mol L^{-1} H_2SO_4, and the right reservoir was filled with 1.5 mol L^{-1} $MgSO_4$ in 3 mol L^{-1} H_2SO_4; the effective area exposed to the solutions was 9 cm^2. The two solutions were both stirred continuously at room temperature. Samples of the $MgSO_4$ solution were withdrawn at regular time intervals and analyzed for VO^{2+} using a UV−vis spectrometer. Assuming that the change of VO^{2+} concentration in the left reservoir is negligible, the relationship between the VO^{2+} concentration in the right reservoir and time follows Fick's diffusion law

Scheme 1. Cell Used for Vanadium Permeation Measurements

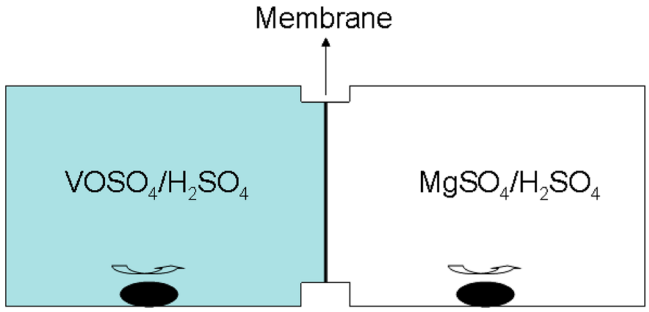

$$V_B \frac{dC_B(t)}{dt} = A\frac{k_D}{l}[C_A - C_B(t)]$$

where V_B is the solution volume in the right reservoir; A and l are the effective area and thickness, respectively, of the membrane; k_D is the diffusion coefficient of VO^{2+}; and C_A and C_B are the VO^{2+} concentrations in the left and right reservoirs, respectively, the latter being a function of time t. This equation can be solved to obtain the diffusion coefficient k_D.

2.3. All-Vanadium Redox Flow Battery (VFB) Performance. A VFB single cell was assembled by sandwiching a membrane with two carbon felt electrodes, clamped by two graphite polar plates and then fixed between two stainless plates. The negative and positive electrolytes were 1.5 M V^{2+}/V^{3+} and 1.5 M VO^{2+}/VO_2^+, respectively, both in 3.0 M H_2SO_4 solution, and they were circulated into the corresponding half-cells. The active area of the cell was 9 cm^2, and the volume of electrolyte solution was 40 mL in each half-cell. Charge−discharge tests were conducted with a constant current density of 80 mA cm^{-2} at room temperature on model BT 2000 apparatus (Arbin Instruments Inc., College Station, TX). The cutoff voltages for charge (upper limit) and discharge (lower limit) were 1.55 and 1.0 V, respectively. The Coulombic efficiency (CE) is defined as the discharge capacity (A h) divided by the charge capacity. Energy efficiency (EE) is defined as the discharge energy (W h) divided by the charge energy. The voltage efficiency (VE) can be calculated as VE = EE/CE.

3. RESULTS AND DISCUSSION

3.1. Fabrication of Prequaternized AEMs. We employed a TEA-enabled prequaternization strategy to fabricate AEMs for VFB use. The fabrication process involves chloromethylation of polysulfone (PSf) with chloromethyl methyl ether, TEA treatment of the chloromethylated PSf (or CMPSf) in a solution, and finally casting of the treated polymer solution for membrane formation. The chloromethylation degree of CMPSf was carefully controlled at around 1.35 so that a good balance between membrane conductivity and mechanical strength could be achieved. TEA treatment of CMPSf was intended for the formation of quaternary ammonium cations through a nucleophilic substitution reaction. Four different solvents were each employed as the medium for this reaction. The treated polymer solution was cast directly and thermally treated to afford the formation of a dried membrane. During this process, a certain degree of microphase separation can be expected. For comparison, an AEM was also fabricated using the postquaternization route, where a preformed CMPSf (with the same chloromethylation degree as above) membrane was treated in TMA (aqueous) to render the membrane functionalized with quaternary ammonium groups. The thickness of each of the membranes was controlled at ca. 60 μm so that a reasonable comparison of their properties could be made.

3.2. Membrane Properties. The physical properties of the fabricated polysulfone AEMs were studied and are compared in Table 1. Among the four TEA-quaternized membranes, the one fabricated from DMSO solvent (AEM1) exhibited much higher water uptake (WU = 23.1%) than those fabricated from DMAc, DMF, and THF (AEM2−AEM4, respectively, displaying WU values of 3.4%, 9.1%, and 2.4% in that order). Meanwhile, AEM1 exhibited an ion-exchange capacity (IEC) of 1.37 mmol g^{-1} and an anionic conductivity of 18.2 mS cm^{-1} at 20 °C, whereas AEM2−AEM4 showed much lower IECs (0.20, 0.19, and 0.15 mmol g^{-1}, respectively) and negligible conductivities. These comparisons reveal that quaternization is significant in DMSO but not in the other solvents. Considering that the high IEC and conductivity of an AEM are essential to guarantee the high energy storage efficiency of a VFB, our results suggest that DMSO is a favorable solvent for VFB membrane fabrication through TEA-enabled prequaternization whereas the other three solvents are not suitable for such a fabrication strategy. Note that the conductivity of AEM1 is relatively low compared to that of Nafion212 (83 mS/cm at 20 °C); this is mainly because the latter transports protons whereas the former conducts anions, whose hydration radius is larger than that of

Table 1. Properties of AEMs Obtained with Different Fabrication Schemes, Quaternization Reagents, and Solvents

sample	fabrication scheme	aminating agent	solvent	WU (%)	IEC(mmol g^{-1})	σ^a (mS cm^{-1})
AEM1	prequaternization	TEA	DMSO	23.1	1.37	18.2
AEM2			DMAc	3.4	0.20	ND[b]
AEM3			DMF	9.1	0.19	ND[b]
AEM4			THF	2.4	0.15	ND[b]
AEM5	postquaternization	soaking in TMA (aqueous)		42.6	1.43	17.1

[a]σ = Conductivity at 20 °C. [b]ND = no reliable results could be detected (impedance close to or larger than that of DI water where the measurement was made).

dx.doi.org/10.1021/jp304880r | J. Phys. Chem. B 2012, 116, 9016−9022

protons. Despite the lower conductivity compared with Nafion212, AEM1 can still a yield high energy efficiency for a VFB because of the resulting low vanadium crossover, as shown in section 3.5.

It is more interesting that AEM1 (from DMSO) displayed a higher conductivity (18.2 versus 17.1 mS/cm) but a lower IEC (1.37 versus 1.43 mmol/g) than the postquaternized AEM5 (from aqueous TMA). This is probably because the prequaternization route led to a high degree of microphase segregation in AEM1, which can form wide and continuous channels for ion transport. The microphase-separated morphology can be observed clearly from the transmission electron microscopy (TEM) image shown in Figure 1a, where the dark

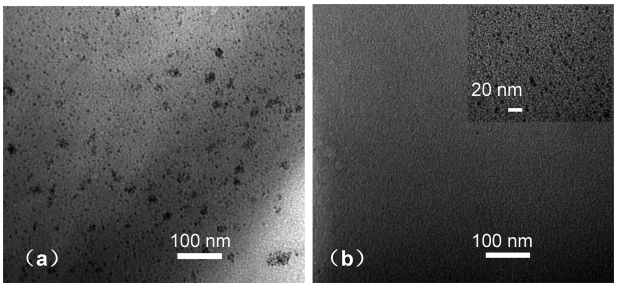

Figure 1. TEM images of (a) AEM1 (prequaternized with TEA using DMSO as the solvent) and (b) AEM5 (postquaternized with aqueous TMA). Inset: Magnified view of image b.

spots represent domains or clusters of hydrophilic quaternary ammonium groups that have been stained with H_2PdCl_4 whereas the light-gray areas are the hydrophobic polymer backbones. In contrast, the TMA-enabled postquaternized membrane (AEM5) shows virtually undetectable microphase separation according to its TEM image (Figure 1b). This is because, in the postquaternization route, the membrane was formed before being rendered into ionic form, and thus, the polymer chain sections cannot aggregate to form ionic clusters. The TEM results in Figure 1 constitute direct and clear evidence that prequaternization promotes microphase aggregation in AEMs.

3.3. Proposed Solvent Effect on TEA-Enabled Prequaternization of CMPSf. It has been reported that, in the fabrication of proton-exchange membranes, certain solvents can undergo strong hydrogen bonding with the $-SO_3H$ group of presulfonated polymers and influence the resulting membranes' conductivities.[36,37] In the present work, we studied AEMs that were prepared by prequaternization of CMPSf with TEA in the presence of different solvents. Interestingly, significant differences were also observed among the resultant AEMs regarding membrane properties (Table 1). To account for such differences, we propose that some of the solvents employed might have competed with TEA to interact with the chloromethyl groups ($-CH_2Cl$) of the polymer, hindering the target reaction between TEA and $-CH_2Cl$ and therefore leading to low levels of polymer quaternization.

To be specific, DMAc is nucleophilic to some degree because its nitrogen atom bears lone-pair electrons (despite being partially delocalized with the carbonyl group) and its three methyl groups are electron-donating. Therefore, donor–acceptor complexation can take place between DMAc and the $-CH_2Cl$ group such that CMPSf quaternization with TEA is hampered. When the TEA-treated polymer solution, presumably containing a $-CH_2^{\delta+}(TEA)(DMAc)Cl^{\delta-}$ intermediate (Scheme 2a), is cast and thermally treated for membrane

Scheme 2. (a) DMAc Competing with TEA to Interact with the Chloromethyl Groups of CMPSf and (b) No Interaction between DMSO and Chloromethyl Groups

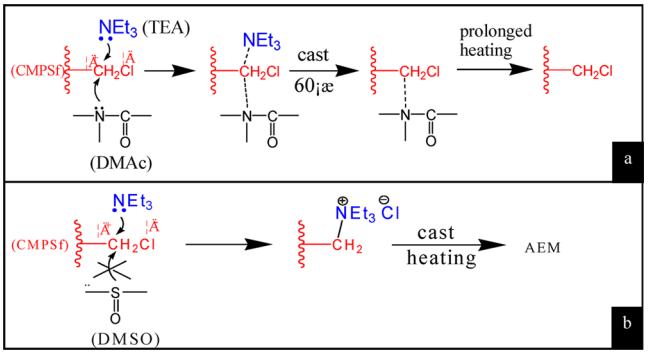

formation, TEA will evaporate first because of its higher volatility and lower boiling point than DMAc, whereas the latter will remain chemically bound to the $-CH_2Cl$ group (Scheme 2a). These events can also happen with DMF (structurally similar to DMAc), which is also an electron donor (although weak) and thus can hinder the target quaternization reaction. In the case of THF, the ether oxygen makes this solvent electron-donating as well, and thus, it can also impede TEA quaternization of CMPSf.

Unlike for DMAc, DMF, and THF, when DMSO is employed as the solvent for the prequanternization reaction, the proposed solvent–TEA competition does not occur to any appreciable extent. This is because the sulfoxide group is electron-withdrawing, and thus, DMSO has a low propensity to react with the $-CH_2Cl$ group (Scheme 2b). As a result, the quaternization reaction of the polymer CMPSf with TEA can proceed free of solvent intervention and thus to a significant level.

3.4. Physical and Chemical Investigations of the Solvent Effect. *3.4.1. Solvent Effect Observed during CMPSf Solution Casting.* The proposed solvent effect can be observed directly from the different casting behaviors of CMPSf solutions made with DMSO and DMAc. Note that neither solution contained any TEA as the quaternization reagent. The CMPSf–DMSO solution became whitish and turbid (Figure 2A) 30 min after casting, indicating CMPSf precipitation by the ambient water vapor. The cast CMPSf–DMAc liquid layer, however, was transparent (Figure 2B) even after 30 min of exposure to the ambient, implying that an interaction between DMAc and CMPSf might have arisen and made the latter more compatible with the ambient water vapor such that no precipitation occurred. The cast DMF and THF solutions were also transparent (not shown separately) after being exposed to the open air for 30 min.

3.4.2. Solvent Effect Detected from Pure CMPSf Membranes without Quaternization. To acquire more enlightening insight into the proposed solvent effect, FTIR spectra (Figure 3) were recorded for the dried CMPSf membranes cast with different solvents (no TEA treatment), all of which underwent a prolonged thermal treatment (60 °C for 24 h). The membrane cast from DMAc exhibited a clear tertiary amide band at around 1640 cm^{-1}(curve A) due to the existence of DMAc, suggesting that a chemical interaction occurred between

dx.doi.org/10.1021/jp304880r | J. Phys. Chem. B 2012, 116, 9016–9022

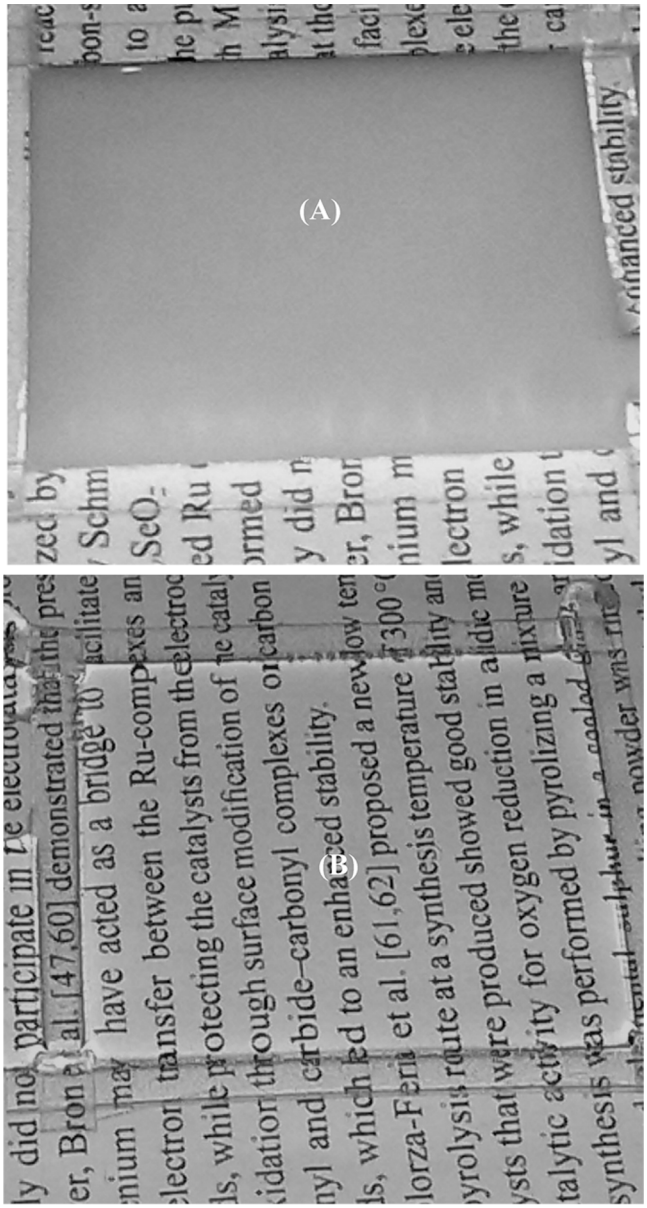

Figure 2. Photographs of casted CMPSf solution with (A) DMSO and (B) DMAc as the solvent, taken 30 min after casting. TEA was not added to these solutions.

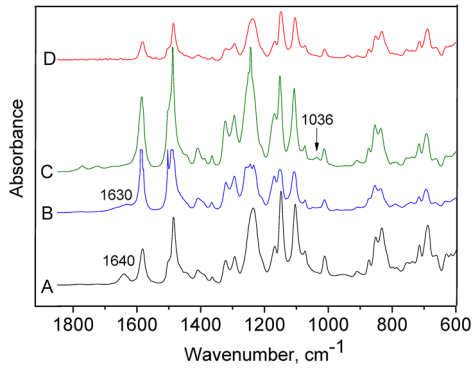

Figure 3. FTIR spectra of CMPSf membranes cast from (A) DMAc, (B) DMF, (C) THF, and (D) DMSO solutions after a 24-h thermal treatment at 60 °C. No TEA treatment was involved.

CMPSf and DMAc and made the latter remain in the final membrane even after a prolonged thermal treatment. The 1640 cm^{-1} band disappeared, and a new band at ca. 1718 cm^{-1} arose (Figure 4) after the membrane was further treated under a

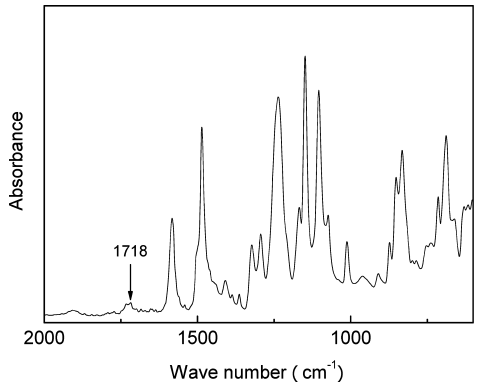

Figure 4. FTIR spectrum of the CMPSf membrane cast from DMAc solution and vacuum-dried at 100 °C for 12 h. No TEA treatment was involved.

vacuum at 100 °C for 12 h, probably due to oxidation of the carbonyl group (with the trace amount of oxygen). Similarly, in the spectra for membranes cast from DMF and THF (curves B and C), characteristic bands attributable to amide (ca. 1630 cm^{-1}) and ether (1036 cm^{-1}) moieties, respectively, were detected, again suggesting that the solvents bonded with CMPSf through a donor−acceptor effect.

In contrast, the membrane cast from DMSO did not show appreciable solvent signals (1030−1060 cm^{-1} for the sulfoxide group) in its FTIR spectrum (curve D in Figure 3), indicating that no interaction between CMPSf and DMSO occurred and that the latter evaporated completely upon prolonged thermal treatment; further vacuum heating at 100 °C did not create any change in this membrane. Note that all of the membranes studied in Figure 3 were made in an identical way except for the choice of solvent; however, they showed clearly different FTIR features. This leads to the conclusion that the solvents indeed interact differently with CMPSf: Those that are relatively more nucleophilic (DMAc, DMF, and THF) interact more strongly than the less nucleophilic solvent (DMSO). Such a difference will result in the failure or success of polymer prequaternization with TEA.

3.4.3. Solvent Effect Observed from TEA-Treated CMPSf Membranes. The FTIR spectra for the dried membranes cast from DMAc, DMF, and THF solutions of CMPSf with or without TEA treatment are compared in Figure 5. In all three comparison groups (A−C), the absorption signals are almost the same for membranes formed with or without TEA treatment of the polymer, meaning that TEA quaternization did not take place to an appreciable level. This further corroborates the suggested solvent effect. It is also interesting to note that a broad band centered around 3360 cm^{-1} is present in both curves B1 and B2; such a band can originate from the hydroxyl group that is produced by another manner of reaction between DMF and the $-CH_2Cl$ group, as reported elsewhere.[38] This occurrence can explain the relatively higher WU value (due to hydrophilicity of hydroxyl group) of AEM3 compared with AEM2 and AEM4 (Table 1).

Figure 6 shows the FTIR spectrum for the dried membrane cast from TEA-treated CMPSf solution in DMSO, namely,

dx.doi.org/10.1021/jp304880r | J. Phys. Chem. B 2012, 116, 9016−9022

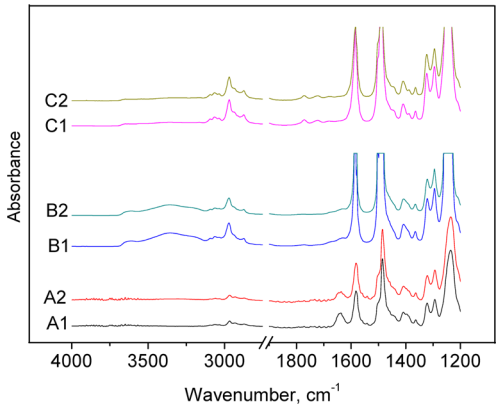

Figure 5. FTIR spectra of membranes cast from (1) pure and (2) TEA-treated CMPSf solutions in (A) DMAc, (B) DMF, and (C) THF.

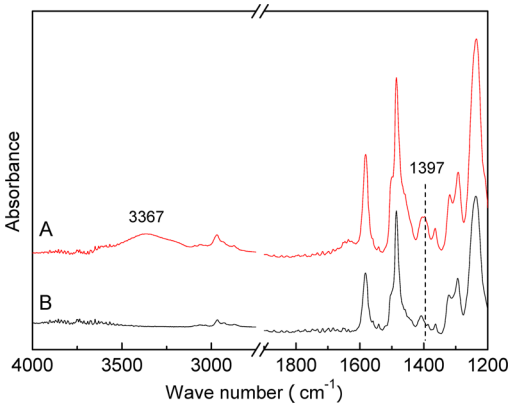

Figure 6. FTIR spectra of (A) a membrane cast from TEA-treated DMSO solution of CMPSf (AEM1) and (B) a pure CMPSf membrane cast from DMSO solution.

AEM1 (curve A), in comparison with that of a pure CMPSf membrane also cast from DMSO solution without TEA treatment (curve B). Sharply different from Figure 5, clear bands at 1397 and 3367 cm^{-1}, associated with quaternary ammonium and its bound water, respectively, can be seen in curve A but not in curve B; this observation confirms that quaternary amination has taken place successfully in the DMSO solution.

3.5. VFB Performance of the TEA-Quaternized AEMs. We have shown that DMSO is a favorable solvent for TEA quaternization of CMPSf and that the resulting membrane (AEM1) exhibits good ion-exchange properties. To further demonstrate the successful fabrication and usefulness of this membrane, we assembled a VFB and studied its battery performance. Figure 7A shows the Coulombic efficiency (CE), energy efficiency (EE), and voltage efficiency (VE) of the battery assembled (AEM1-VFB), which experienced 80 charge–discharge cycles at a current density of 80 mA cm^{-2}. Its efficiencies were stable during these cycles, with CE and EE averaging 99% and 81%, respectively. For comparison, we also constructed a VFB using a Nafion212 membrane (with a thickness similar to that of AEM1). This battery (Nafion212-VFB) yielded a CE of 94–95% and an EE of 81–82% over 22 cycles also at 80 mA cm^{-2} (as shown in Figure 7B). Apparently, the AEM1-VFB is advantageous over the Nafion212-VFB in terms of Coulombic efficiency. This feature endows the AEM1-

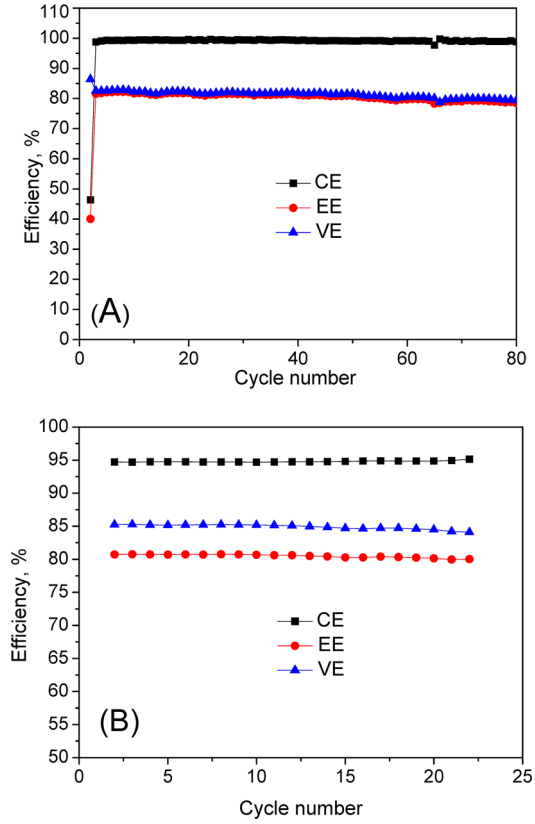

Figure 7. Efficiencies of (A) AEM1-VFB and (B) Nafion212-VFB operating at 80 mA cm^{-2} and room temperature.

VFB with a high EE that is comparable to that of Nafion-assembled VFB even though AEM1 is less conductive than Nafion. In fact, literature reporting EE values above 80% at 80 mA cm^{-2} is very rare. To the best of our knowledge, our work represents the first example of a TEA-quaternized AEM application in a VFB showing a high efficiency of energy storage. We also tried the other three TEA-quaternized membranes (AEM2–AEM4) for VFB application, but they failed to enable normal charge/discharge operation because of ion-exchange capacities and conductivities that were too low, as shown in Table 1.

The higher CE of AEM1-VFB compared to Nafion212-VFB can be explained as follows: AEM1 carries positive charges due to the presence of quaternary ammonium cations on its molecular chains. This feature allows transport of anions (SO_4^{2-} and HSO_4^-) through the membrane to achieve charge balance during battery operation and meanwhile repulses the vanadium ions (also positively charged) due to Donnan effect. On the contrary, the Nafion membrane is negatively charged due to the existence of sulfonate groups ($-SO_3H$) and thus can transport both protons and vanadium ions, although vanadium transport is minor compared with proton transport because of the size effect; such vanadium diffusion across the membrane will result in lowered Coulombic efficiency. The better vanadium repulsion of AEM1 compared with Nafion212 can be seen from a comparison of their VFB self-discharge (caused by vanadium crossover) behaviors shown in Figure 8, where the AEM1-VFB displayed a much longer self-discharge time (ca. 100 h) than the Nafion212-VFB (ca. 40 h). This is further confirmed by the significantly lower vanadium permeability of

dx.doi.org/10.1021/jp304880r | J. Phys. Chem. B 2012, 116, 9016–9022

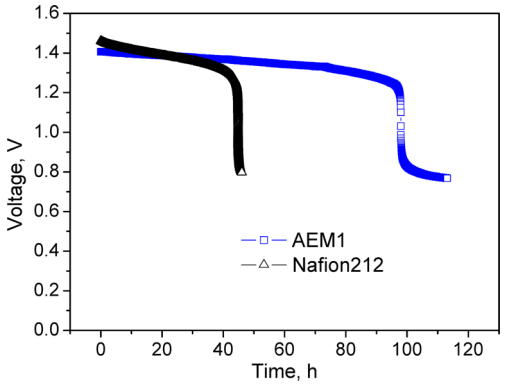

Figure 8. Self-discharge curves of AEM1-VFB and Nafion212-VFB.

AEM1 (1.6×10^{-8} cm^2/min) compared with that of Nafion212 (1.1×10^{-7} cm^2/min).

4. CONCLUSIONS

In summary, we have investigated the solvent effect on the TEA-enabled prequaternization of polysulfone for AEM fabrication. Our results reveal that DMSO is a good solvent for the above process, whereas DMAc, DMF, and THF are not recommended because of their electron-donation nature leading to solvent−TEA competition during the quaternization reaction. The membrane fabricated from DMSO exhibited high ion-exchange capacity and conductivity as well as promising VFB performance (high Coulombic and energy efficiencies). Our work provides direct evidence for membrane microphase separation promoted by prequaternization and adds new understanding to the quaternization chemistry of AEMs. It is also the first demonstration, to our knowledge, of TEA-quaternized AEMs utilized in VFB and showing high efficiencies and good durability.

AUTHOR INFORMATION

Corresponding Author

*Tel.: 86-411-84379669 (F.Z.), 86-411-84379072 (H.Z.). Fax: 86-411-84665057 (F.Z.), 86-411-84665057 (H.Z.). E-mail: zhfx2003@hotmail.com (F.Z.), zhanghm@dicp.ac.cn (H.Z.).

Notes

The authors declare no competing financial interest.

ACKNOWLEDGMENTS

This work was financially supported by the 100-Talent Program of Dalian Institute of Chemical Physics, Chinese Academy of Sciences; National Basic Research Program of China (Grant 2010CB227202); Natural Scientific Foundation of Liaoning Province, China (Grant 20102226); and Science Fund of Dalian, China (Grant 2011J21DW026)

REFERENCES

(1) Li, X. F.; Zhang, H. M.; Mai, Z. S.; Zhang, H. Z.; Vankelecom, I. *Energy Environ. Sci.* **2011**, *4*, 1147−1160.
(2) Chen, D. Y.; Wang, S. J.; Xiao, M.; Meng, Y. Z. *J. Power Sources* **2010**, *195*, 2089−2095.
(3) Kim, S.; Yan, J. L.; Schwenzer, B.; Zhang, J. L.; Li, L. Y.; Liu, J.; Yang, Z. G.; Hickner, M. A. *Electrochem. Commun.* **2010**, *12*, 1650−1653.
(4) Chen, D. Y.; Wang, S. J.; Xiao, M.; Han, D. M.; Meng, Y. Z. *J. Power Sources* **2010**, *195*, 7701−7708.
(5) Jia, C. K.; Liu, J. G.; Yan, C. W. *J. Power Sources* **2010**, *195*, 4380−4383.
(6) Luo, Q. T.; Zhang, H. M.; Chen, J.; Qian, P.; Zhai, Y. F. *J. Membr. Sci.* **2008**, *311*, 98−103.
(7) Luo, Q. T.; Zhang, H. M.; Chen, J.; You, D. J.; Sun, C. X.; Zhang, Y. *J. Membr. Sci.* **2008**, *325*, 553−558.
(8) Mai, Z. S.; Zhang, H. M.; Li, X. F.; Bi, C.; Dai, H. *J. Power Sources* **2011**, *196*, 482−487.
(9) Zhang, H.; Zhang, H.; Li, X.; Mai, Z.; Zhang, J. *Energy Environ. Sci.* **2011**, *4*, 1676−1679.
(10) Xing, D. B.; Zhang, S. H.; Yin, C. X.; Zhang, B. G.; Jian, X. G. *J. Membr. Sci.* **2010**, *354*, 68−73.
(11) Zhang, S. H.; Yin, C. X.; Xing, D. B.; Yang, D. L.; Jian, X. G. *J. Membr. Sci.* **2010**, *363*, 243−249.
(12) Zeng, Q. H.; Liu, Q. L.; Broadwell, I.; Zhu, A. M.; Xiong, Y.; Tu, X. P. *J. Membr. Sci.* **2010**, *349*, 237−243.
(13) Xiong, Y.; Liu, Q. L.; Zeng, Q. H. *J. Power Sources* **2009**, *193*, 541−546.
(14) Varcoe, J. R.; Slade, R. C. T.; Lam How Yee, E.; Poynton, S. D.; Driscoll, D. J.; Apperley, D. C. *Chem. Mater.* **2007**, *19*, 2686−2693.
(15) Kumar, M.; Singh, S.; Shahi, V. K. *J. Phys. Chem. B* **2010**, *114*, 198−206.
(16) Slade, R. C. T.; Varcoe, J. R. *Solid State Ionics* **2005**, *176*, 585−597.
(17) Hibbs, M. R.; Fujimoto, C. H.; Cornelius, C. J. *Macromolecules* **2009**, *42*, 8316−8321.
(18) Herman, H.; Slade, R. C. T.; Varcoe, J. R. *J. Membr. Sci.* **2003**, *218*, 147−163.
(19) Fang, J.; Shen, P. K. *J. Membr. Sci.* **2006**, *285*, 317−322.
(20) Danks, T. N.; Slade, R. C. T.; Varcoe, J. R. *J. Mater. Chem.* **2003**, *13*, 712−721.
(21) Zhang, F. X.; Zhang, H. M.; Ren, J. X.; Qu, C. *J. Mater. Chem.* **2010**, *20*, 8139−8146.
(22) Wang, J.; Zhao, Z.; Gong, F.; Li, S.; Zhang, S. *Macromolecules* **2009**, *42*, 8711−8717.
(23) Schmidt-Rohr, K.; Chen, Q. *Nat. Mater.* **2008**, *7*, 75−83.
(24) Park, C. H.; Lee, C. H.; Sohn, J.-Y.; Park, H. B.; Guiver, M. D.; Lee, Y. M. *J. Phys. Chem. B* **2010**, *114*, 12036−12045.
(25) Jang, S. S.; Lin, S.-T.; Çağın, T.; Molinero, V.; Goddard, W. A. *J. Phys. Chem. B* **2005**, *109*, 10154−10167.
(26) Cui, S.; Liu, J.; Selvan, M. E.; Keffer, D. J.; Edwards, B. J.; Steele, W. V. *J. Phys. Chem. B* **2007**, *111*, 2208−2218.
(27) Bae, B.; Miyatake, K.; Watanabe, M. *ACS Appl. Mater. Interfaces* **2009**, *1*, 1279−1286.
(28) Liu, J.; Wang, H.; Cheng, S.; Chan, K. Y. *Chem. Commun.* **2004**, 728−729.
(29) Zhang, Q.; Li, S.; Zhang, S. *Chem. Commun.* **2010**, *46*, 7495−7497.
(30) Hall, H. K. *J. Am. Chem. Soc.* **1957**, *79*, 5441−5444.
(31) Wang, G.; Weng, Y.; Chu, D.; Chen, R.; Xie, D. *J. Membr. Sci.* **2009**, *332*, 63−68.
(32) Vinodh, R.; Ilakkiya, A.; Elamathi, S.; Sangeetha, D. *Mater. Sci. Eng. B* **2010**, *167*, 43−50.
(33) Wu, Y. H.; Wu, C. M.; Xu, T. W.; Lin, X. C.; Fu, Y. X. *J. Membr. Sci.* **2009**, *338*, 51−60.
(34) Wu, Y. H.; Wu, C. M.; Varcoe, J. R.; Poynton, S. D.; Xu, T. W.; Fu, Y. X. *J. Power Sources* **2010**, *195*, 3069−3076.
(35) Zhang, F.; Zhang, H.; Qu, C. *J. Mater. Chem.* **2011**, *21*, 12744−12752.
(36) Robertson, G. P.; Mikhailenko, S. D.; Wang, K.; Xing, P.; Guiver, M. D.; Kaliaguine, S. *J. Membr. Sci.* **2003**, *219*, 113−121.
(37) Guan, R.; Dai, H.; Li, C.; Liu, J.; Xu, J. *J. Membr. Sci.* **2006**, *277*, 148−156.
(38) Alexandratos, S. D.; Zhu, X. *Macromolecules* **2003**, *36*, 3436−3439.